Microchimica Acta (2019) 186: 630
https://doi.org/10.1007/s00604-019-3744-7

ORIGINAL PAPER

Core-shell upconversion nanoparticles of type $NaGdF_4$:Yb,Er@$NaGdF_4$:Nd,Yb and sensitized with a NIR dye are a viable probe for luminescence determination of the fraction of water in organic solvents

Wen Wang[1] · Mingying Zhao[1] · Lun Wang[1] · Hongqi Chen[1]

Received: 13 April 2019 / Accepted: 10 August 2019 / Published online: 17 August 2019

Abstract

Lanthanide-doped core-shell upconversion nanoparticles (UCNPs) of type $NaGdF_4$:Yb,Er@$NaGdF_4$:Yb,Nd were prepared by the co-precipitation method. The luminescence intensity was further enhanced by adding the sensitizer dye IR-808. If water is added to organic solvents [such as N,N-dimethylformamide (DMF), dimethyl sulfoxide, methanol, acetone, acetonitrile, and ethanol] containing the probe, its luminescence intensity peaking at 545 nm is reduced. The decrease is linearly related to the percentage of water in the respective organic solvent. Water fractions ranging from 0.05% to 10% (volume %) can be sensitively detected, and the detection limit is 0.018% of water in DMF. The detection scheme is mainly attributed to the fact that the transfer of energy from the near-infrared light (NIR) dye to the UCNPs is strongly reduced in the presence of traces of water.

Keywords Upconversion nanoparticles · Dye sensitization · Luminescent probe · Water fraction

Introduction

Water in organic solvents usually has a strong and often adverse effect on organic chemical reactions. Even a small amount of water in drugs, fuels and lubricants can cause considerable damage [1–3]. Therefore, the detection of water is significant not only for basic research but also for many application prospects, such as in the pharmaceutical, chemical and petrochemical fields. To date, various techniques have been developed to detect water, including optical-fiber sensor detection [4, 5], fluorescence [6, 7], light-emitting sensor detection [8, 9] and photoinduced electron transfer [10] methods to replace the standard Karl Fischer titration [11] and gas chromatography [12]. Among these water detection methods, optical sensor detection has attracted attention because of its advantages of high efficiency, rapidity, simplicity and sensitivity, and the sensitivity of the fluorescent sensor to detect water in the organic phase has reached the ppm level. Despite these improvements, there are still many problems, such as low repeatability [13], which greatly limits the application of these methods in water detection.

Lanthanide-doped UCNPs have attracted increasing interest because of their distinctive properties. These properties include chemical and optical stability, narrow emission peaks, low spontaneous fluorescence backgrounds, low toxicity, large anti-Stokes shifts and long fluorescence lifetimes [14]. These particles can convert NIR into ultraviolet and visible light and have the ability to penetrate deep tissue. Therefore, lanthanide-doped UCNPs have been widely used in bioimaging [15], cancer treatment [16], drug delivery [17, 18] and photodynamic therapy [19–21]. However, the weak,

Electronic supplementary material The online version of this article (https://doi.org/10.1007/s00604-019-3744-7) contains supplementary material, which is available to authorized users.

✉ Lun Wang
wanglun@mail.ahnu.edu.cn

✉ Hongqi Chen
hq80chen@mail.ahnu.edu.cn

[1] Anhui Key Laboratory of Chemo-Biosensing, Key Laboratory of Functional Molecular Solids, Ministry of Education, College of Chemistry and Materials Science, Anhui Normal University, Wuhu 241000, People's Republic of China

narrow-band NIR absorption of UCNPs limits the photon capture capability of UCNPs, greatly suppressing the upconversion luminescence (UCL) intensity [22]. To enhance the luminescence intensity of UCNPs, NIR dyes can be used to sensitize UCNPs [23–26]. Based on the above problems, designing and synthesizing UCNPs with high emissivity and high conversion efficiency is vital for the water sensing platform.

Herein, a material consisting of $NaGdF_4$:Yb,Er@$NaGdF_4$:Yb,Nd nanoparticles with dye-sensitized nanoprobe for the measurement of water content in several kinds of organic solvents was developed. Because the sensitization efficiency of dyes in water is far below that in organic phase, the luminescence intensity of the system is quenched. The relationship between the reduction in luminescence intensity and water content is deduced to achieve the sensitive detection of water.

Experimental

Conjugation of the IR-808 dye to the surface of core-shell UCNPs

The ligand exchange method was used to prepare IR-808-sensitized UCNPs. Briefly, 1 mL of a solution of UCNPs (5 $g{\cdot}L^{-1}$) modified with nitrosyl tetrafluoroborate ($NOBF_4$) was mixed with 10 μL of IR-808 (1 $g{\cdot}L^{-1}$) in DMF solution, and the mixture was gently shaken at room temperature for 2 h to acquire IR-808-UCNPs. Finally, centrifugation yielded a solid product.

Water determination in organic solvents

The Dye-UCNPs solid prepared above was dissolved by adding 1 mL of DMF, and the same Dye-UCNPs liquid was taken and different amounts of water were added. Then, the samples were diluted to 1 mL with DMF and shaken at room temperature for 30 min. The emission peak at 500 to 580 nm was recorded in a quartz cuvette under laser excitation at 808 nm. The tests for water in DMSO, methanol, acetone, acetonitrile and EtOH were performed in a similar manner.

Results and discussion

Characterization

To study the possibility of using dye-sensitized UCNPs to detect water content, oleic acid-terminated $NaGdF_4$:Yb,Er@$NaGdF_4$:Yb,Nd UCNPs were prepared by co-precipitation. As shown in Fig. 1, $NaGdF_4$:Yb,Er nanoparticles and $NaGdF_4$:Yb,Er@$NaGdF_4$:Yb,Nd nanoparticles had uniform morphology and were well dispersed. The particle size of $NaGdF_4$:Yb,Er@$NaGdF_4$:Yb,Nd UCNPs (average size of ~20 nm) is significantly increased compared to that of $NaGdF_4$:Yb,Er (average size of ~13 nm). The characteristic peak of Nd^{3+} appeared in the EDX spectrum, as shown in Fig. S1b, indicating that UCNPs with core-shell structures were successfully synthesized. The XRD pattern shows that the peaks positions and intensities of $NaGdF_4$:Yb,Er@$NaGdF_4$:Yb,Nd UCNPs were closely matched with the standard JCPDS27–0699 (Fig. S2) [27].

IR-808 was prepared by nucleophilic substitution of the chlorine atom in IR-783 (Scheme S1). The absorption spectra of IR-783 and IR-808 in DMF are shown in Fig. S3. The maximum absorption peaks of IR-783 and IR-808 in DMF are located at 793 nm and 808 nm. It can be seen that a significant redshift has occurred. Combined with the mass spectrum, IR-808 was successfully prepared (MS: calculated for $C_{45}H_{51}O_8S_3N_2Na$: 867.2778, found 867.2634) (Fig. S4). Its maximum absorption occurs at a wavelength of 808 nm, so it is denoted IR-808.

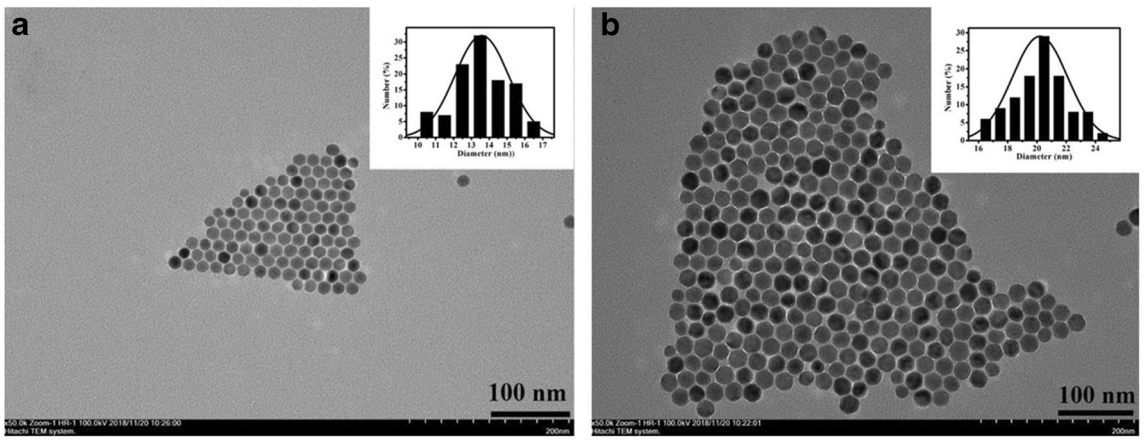

Fig. 1 TEM images of $NaGdF_4$:Yb,Er (**a**) and $NaGdF_4$:Yb,Er@$NaGdF_4$:Yb,Nd (**b**). The inset shows the size distributions of UCNPs

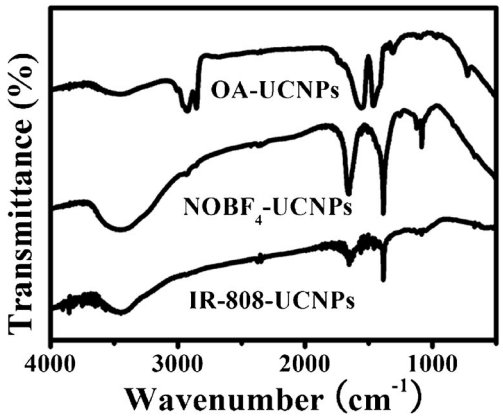

Fig. 2 FT-IR spectra of the OA-UCNPs, $NOBF_4$-UCNPs and IR-808- UCNPs

The original oleic (OA) acid ligand was replaced BF_4^- ligand and then further exchanged with a carboxyl-functionalized IR-808. Fourier transform infrared spectroscopy was used to characterize the modified material. As show in Fig. 2, the absorption peaks of OA-coated UCNPs appeared at 1458 and 1554 cm^{-1} and were attributed to the carboxyl group. The peaks at 2856 and 2929 cm^{-1} are due to -CH asymmetric and symmetric vibrations. The broad absorption peak at 3435 cm^{-1} is due to the vibration of O-H. In the spectra of UCNPs modified with $NOBF_4$, the intensity of the peak due to the C-H stretching vibration of OA at 2800–3000 cm^{-1} was significantly reduced. In addition, the intensity of the carboxyl vibration peak at 1500–1200 cm^{-1} was also greatly reduced, while the vibration peak attributed to $NOBF_4$ appeared at 1084 cm^{-1}. These results indicate that the BF_4^- ligand has successfully replaced the OA ligand on the UCNPs surface. The new peak at approximately 1650 cm^{-1} is caused by the stretching vibration of C=O in DMF. When IR-808 is bound to UCNPs, new peaks appeared at 1000–1500 cm^{-1}, which indicated that the IR-808 dye had been successfully connected to the surface of the $NOBF_4$-UCNPs [27].

Scheme 1 Principle of luminescence determination of water in organic solvents with dye-sensitized UCNPs (Scheme 1d, Dye-UCNPs (red line), Dye-UCNPs-Water (black line))

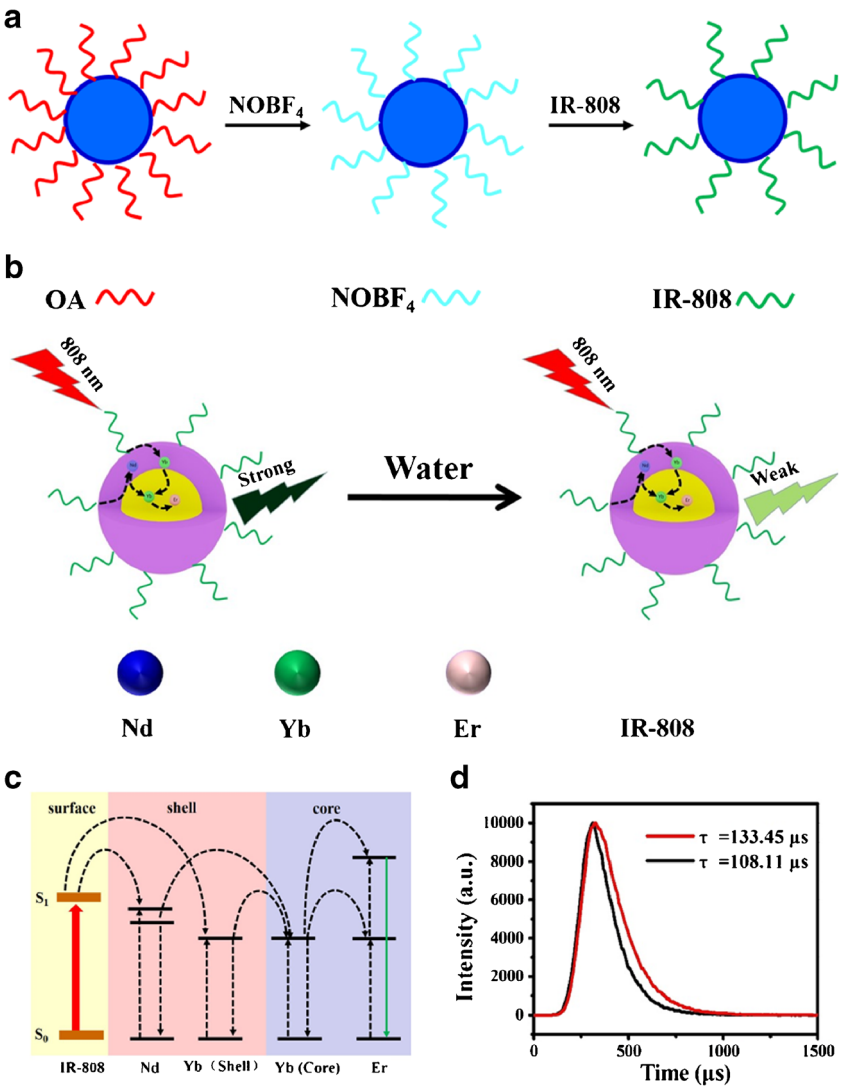

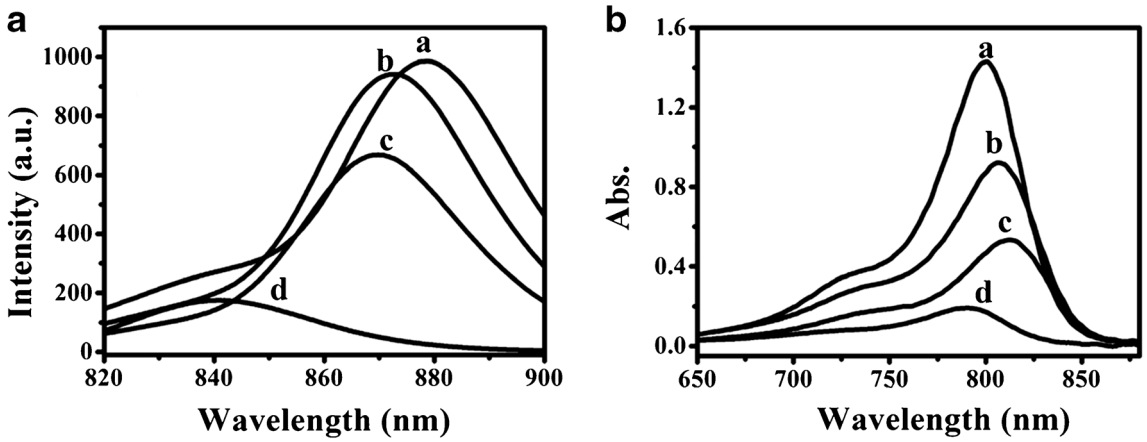

Fig. 3 **a** Fluorescence spectra of IR-808 in DMSO (a), DMF (b), EtOH (c) and H_2O (d) obtained by measuring the absorption from 820 to 900 nm. **b** Absorption spectra of IR-808 in EtOH (a), DMF (b), DMSO (c) and H_2O (d) (concentrations are all 11.54 μM) obtained by measuring the emission from 650 to 870 nm

Principle and mechanism of the nanoprobe

In the first step, the BF_4^- ligand was substituted for the primary OA ligand. In the second step, the BF_4^- ligand was exchanged with IR-808 to achieve Dye-UCNPs in DMF (Scheme 1a) [23]. The IR-808 dye collects photons of approximately 800 and 980 nm and transfers them to the Nd^{3+} and Yb^{3+} (doped in the shell layer) and then to the luminescent Er^{3+} centre by means of the Yb^{3+} ions in the nucleus (shown in Scheme 1b and c) [27]. As shown in Scheme 1d, when water was added to Dye-UCNPs in DMF, the luminescence lifetime of the Dye-UCNPs-Water (black line) became shorter than that of the Dye-UCNPs (red line), indicating that the energy transfer efficiency from the dye to the UCNPs was reduced. To further explore the principle, the same concentration of dye was dissolved in different solvents, and the fluorescence and absorption spectra of these samples were recorded separately (Fig. 3). The absorption and luminescence intensities of the dye in water were far below those in organic solvents. The absorbance of the dye decreased when the dye was bound to UCNPs (Fig. 4a); however, when different volumes of water were introduced into the Dye-UCNPs dispersed in DMF, the absorption of the dye in the supernatant increased (Fig. 4b), indicating that the surface of the IR-808 dye attached to the UCNPs was affected by water. Based on the above facts, the mechanism of this detection is mainly attributed to the amount of NIR dyes adsorbed on the UCNPs surface is affected by water, and the NIR dye transfer efficiency in water is far less than that in the organic phase [26].

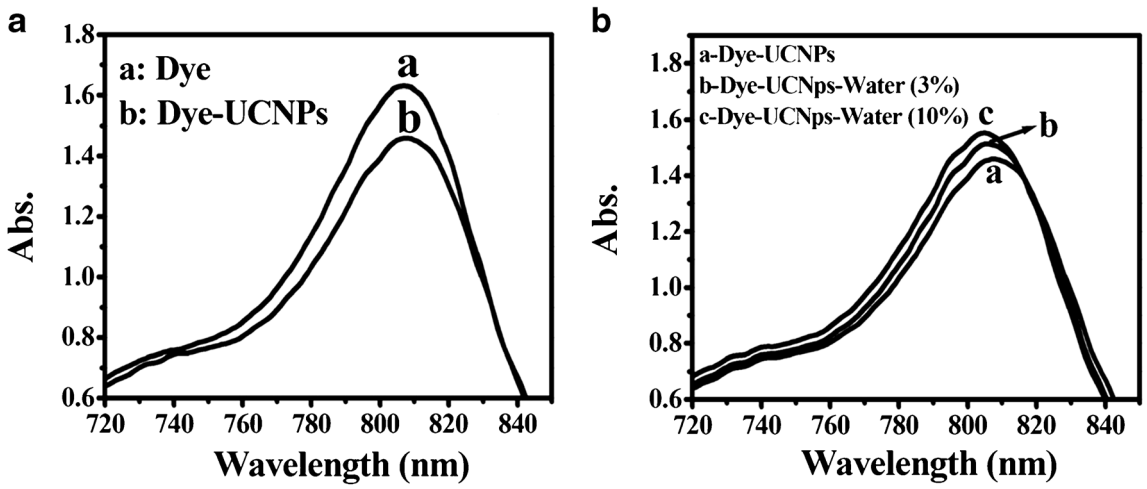

Fig. 4 **a** The change in the absorption spectrum at 808 nm of the Dye (a) and Dye-UCNPs (b) in DMF. **b** Absorption spectra of Dye-UCNPs in DMF (a), DMF with the water content of 3% (b), and DMF with the water content of 10% (c) (The type of dye is IR-808.) obtained by measuring the absorption from 720 to 850 nm

Optimization of experimental conditions

In order to get better experimental results, the following parameters were optimized: (a) Dye type; (b) Dye concentration. Respective data and figures are given in the Electronic Supporting Material (Fig. S5 and Fig. S6). The following experimental conditions were found to give best results: (a) Best dye type: IR-808; (b) Optimal dye concentration: 11.54 μM.

Temperature has a great influence on this method. When the temperature increases gradually, fluorescence quenching will occur (Fig. S7). First, as the temperature increases, the luminous intensity and lifetime of the luminescent material decrease; this phenomenon is called hot quenching. Second, since the population of the thermal coupling energy level always satisfies the Boltzmann distribution during the illumination process, the fluorescence intensity ratio of the two energy levels is dependent on the temperature. The luminescence in-

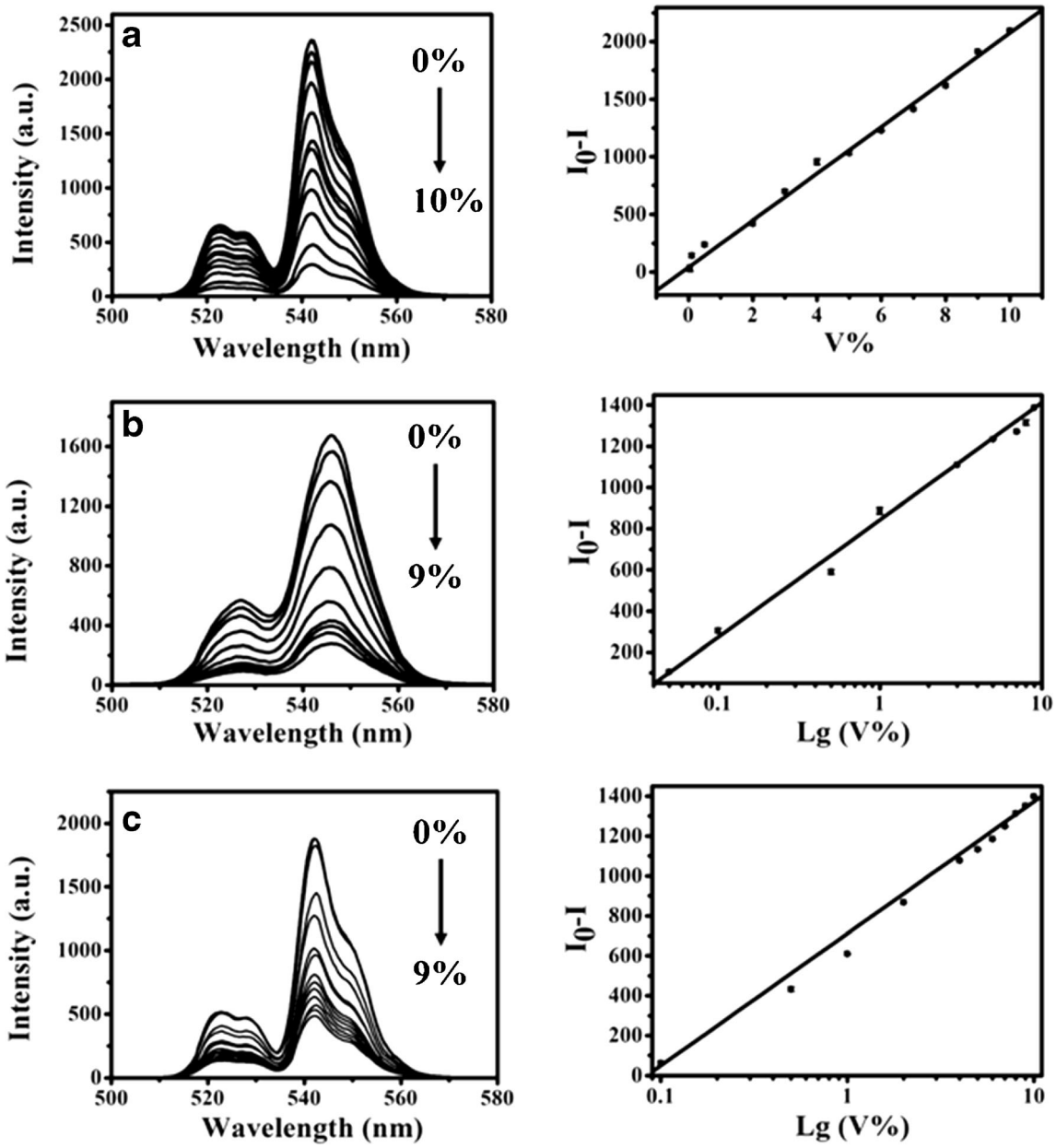

Fig. 5 Upconversion emission changes of Dye-UCNPs as a function of water (volume (V) %) in DMF (**a**). The change in emission peak intensity (I_0-I) at 545 nm is a function of the change in water volume ratio. DMSO (**b**), methanol (**c**), acetone (**d**), acetonitrile (**e**), and EtOH (**f**). The emission intensity was obtained by measuring the emission at 500 to 580 nm (I_0 represents the luminescence intensity of Dye-UCNPs; I represents the luminescence intensity of Dye-UCNPs-Water). The data are expressed as the average of three measurements

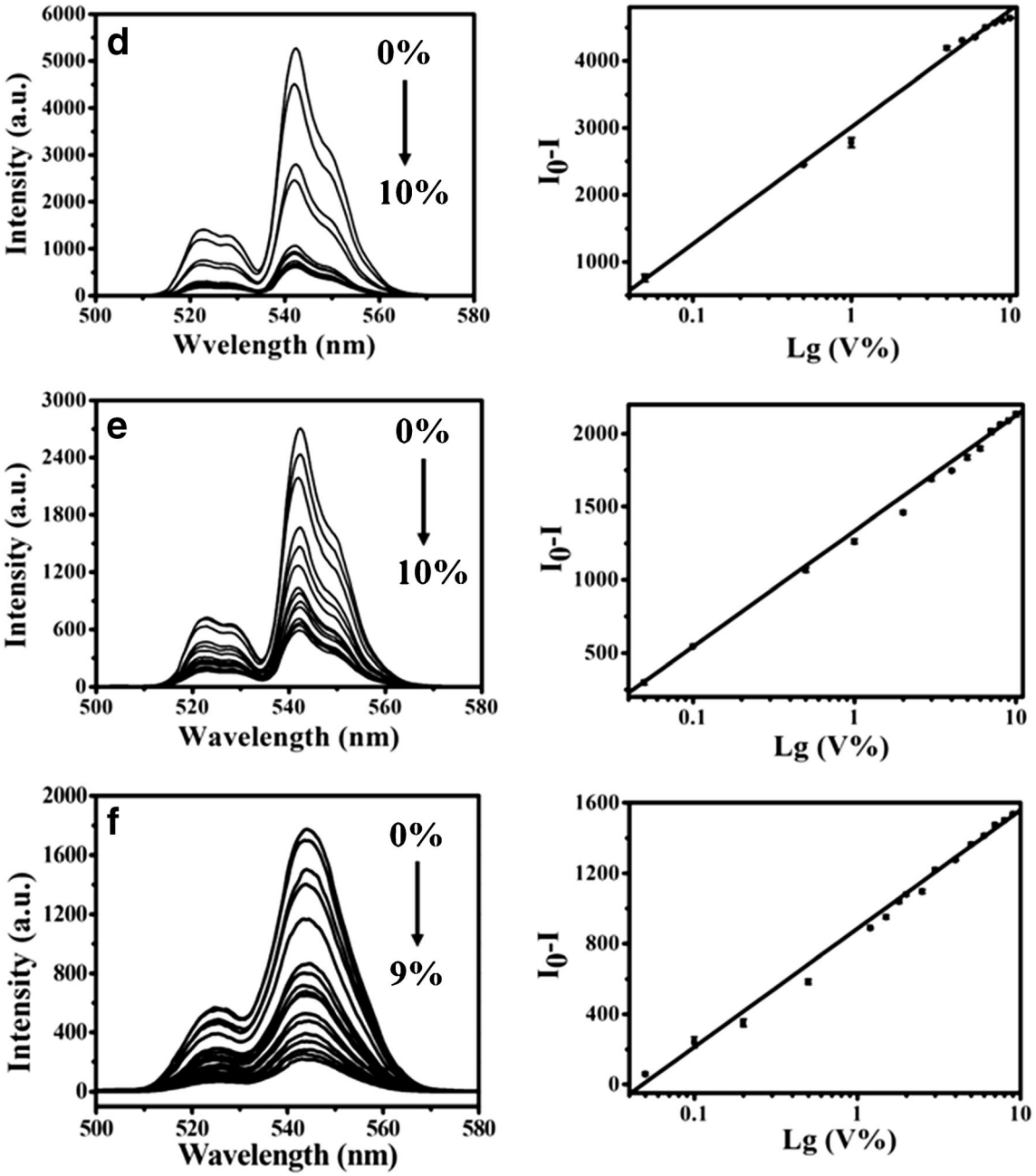

Fig. 5 (continued)

tensity of Yb^{3+} and Er^{3+}-doped UCNPs is greatly affected by temperature. In particular, the ratio between the intensities of the green emission lines at 525 and 545 nm is extremely sensitive to temperature. These two emission lines are attributed to energy-intensive Er^{3+} ion states that are thermally coupled [28]. Therefore, the test process of this experiment was carried out at room temperature.

Detection of moisture in organic solvents

The water indwell in DMF was detected by the IR-808-UCNPs probe. When the water content in the system increased to 10%, the quenching rate reached 87.7%, as shown in Fig. 5a, and when the water content was 0.05%~10% ($R^2 = 0.997$), the decrease in luminescence intensity was linearly related to the percentage of water content and the detection limit is 0.018%. The equation of the calibration plot is I_0-$I = 40.20 + 203.50 \cdot x$ (I_0 represents the luminescence intensity in the absence of water, I is the luminescence intensity when water is added, and x represents the percentage of water volume %). The luminescence spectra and functional relationships of probes for the detection of water content in other organic solvents were obtained (see in Fig. 5). The quenching efficiency of Dye-UCNPs in different solvents

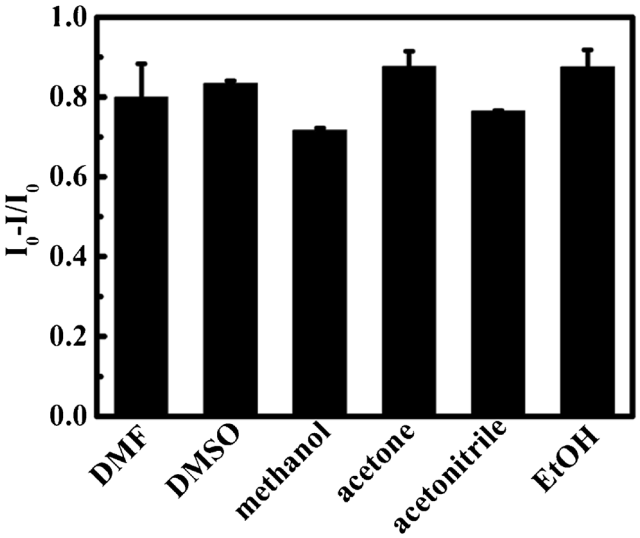

Fig. 6 The quenching efficiency of fluorescence at 545 nm in different solvents when the water content is 9% (I_0 represents the luminescence intensity of Dye-UCNPs, I represents the luminescence intensity of Dye-UCNPs-Water). The data are expressed as the average of three measurements

and the change in fluorescence intensity at 545 nm as a function of water content in the presence of water are given in Fig. 6 and Table S1. The feasibility of applying dye-sensitized nanoprobe in practical specimens was studied. Three actual samples were analysed using Dye-UCNPs nanoprobe, the results are shown in Table 1. The results of the three samples are close to those measured by the Karl Fischer method, and the relative standard deviation (RSD, $n = 3$) is less than 1%. These results clearly show that the IR-808-UCNPs nanoprobe is able to detect water in authentic specimens. Compared with other water probes, this nanoprobe has a wider linear range and a lower detection line (Table S2).

Conclusion

A method is described for the determination of trace water in organic solvents. The method is rapid, convenient and sensitive. IR-808 dye was designed and synthesized and then used to enhance the upconversion luminescence. The detection of trace water in several organic solvents, such as DMF, DMSO, methanol, acetone, acetonitrile and EtOH, were carried out using dye-sensitized $NaGdF_4$:Yb,Er@$NaGdF_4$:Yb,Nd UCNPs as a nanoprobe. The method is temperature sensitve and its resolution ($\Delta S/\Delta conc$) is poor. However, it also has some advantages, such as rapid, convenient and wide range of analysis. This method can be widely applied to the detection of water content in alcohols, ketones and hydrophilic organic solvents. The dye-sensitized UCNPs are expected to be used in water analysis in industrial processes.

Table 1 Detection of water content in samples

Samples	Karl Fischer method (%)	Measure (%)	RSD (n = 3) (%)
EtOH (Corn)	0.25	0.26	0.14
EtOH (95%)	5.58	5.43	0.13
DMF	0.20	0.22	0.49

Acknowledgements This work was financially supported by natural science foundation of China (21675002), the education commission natural science foundation of Anhui Province (KJ2017ZD25), foundation for innovation team of bioanalytical chemistry and Special and Excellent Research Fund of Anhui Normal University.

Compliance with ethical standards The author(s) declare that they have no competing interests.

References

1. Wang L, Li Y (2007) Luminescent coordination compound nanospheres for water determination. Small 3(7):1218–1221. https://doi.org/10.1002/smll.200600564
2. Gao F, Luo F, Chen X, Yao W, Yin J, Yao Z, Wang L (2009) Fluorometric determination of water in organic solvents using europium ion-based luminescent nanospheres. Microchim Acta 166(1–2):163–167. https://doi.org/10.1007/s00604-009-0180-0
3. Kang E, Park HR, Yoon J, Yu H-Y, Chang S-K, Kim B, Choi K, Ahn S (2018) A simple method to determine the water content in organic solvents using the 1 H NMR chemical shifts differences between water and solvent. Microchem J 138: 395–400. https://doi.org/10.1016/j.microc.2018.01.034
4. Ohira S, Miki Y, Matsuzaki T, Nakamura N, Sato YK, Hirose Y, Toda K (2015) A fiber optic sensor with a metal organic framework as a sensing material for trace levels of water in industrial gases. Anal Chim Acta 886:188–193. https://doi.org/10.1016/j.aca.2015.05.045
5. Huang D, Bing Y, Yi H, Hong W, Lai C, Guo Q, Niu C (2015) An optical-fiber sensor based on time-gated fluorescence for detecting water content in organic solvents. Anal Methods 7(11):4621–4628. https://doi.org/10.1039/c5ay00110b
6. Wang X-Y, Niu C-G, Hu L-Y, Huang D-W, Wu S-Q, Zhang L, Wen X-J, Zeng G-M (2017) A fluorescent ratiometric sensor based on covalent immobilization of chalcone derivative and porphyrin zinc for detecting water content in organic solvents. Sensors Actuators B Chem 243:1046–1056. https://doi.org/10.1016/j.snb.2016.12.084
7. Ye C, Qin Y, Huang P, Chen A, Wu FY (2018) Facile synthesis of carbon nanodots with surface state-modulated fluorescence for highly sensitive and real-time detection of water in organic solvents. Anal Chim Acta 1034:144–152. https://doi.org/10.1016/j.aca.2018.06.003
8. Wu JX, Yan B (2017) A dual-emission probe to detect moisture and water in organic solvents based on green-Tb(3+) post-coordinated metal-organic frameworks with red carbon dots. Dalton Trans 46(21):7098–7105. https://doi.org/10.1039/c7dt01352c
9. Zhou Y, Zhang D, Xing W, Cuan J, Hu Y, Cao Y, Gan N (2019) Ratiometric and turn-on luminescence detection of water in organic solvents using a responsive europium-organic framework. Anal Chem 91:4845–4851. https://doi.org/10.1021/acs.analchem.9b00493

10. Chen L, Ye JW, Wang HP, Pan M, Yin SY, Wei ZW, Zhang LY, Wu K, Fan YN, Su CY (2017) Ultrafast water sensing and thermal imaging by a metal-organic framework with switchable luminescence. Nat Commun 8:15985. https://doi.org/10.1038/ncomms15985
11. Dantan N, Frenzel W, Küppers S (2000) Determination of water traces in various organic solvents using Karl Fischer method under FIA conditions. Talanta 52(1):101–109. https://doi.org/10.1016/S0039-9140(00)00328-3
12. Xu BQ, Rao CQ, Cui SF, Wang J, Wang JL, Liu LP (2018) Determination of trace water contents of organic solvents by gas chromatography-mass spectrometry-selected ion monitoring. J Chromatogr A 1570:109–115. https://doi.org/10.1016/j.chroma.2018.07.068
13. Guo S, Xie X, Huang L, Huang W (2016) Sensitive water probing through nonlinear photon Upconversion of lanthanide-doped nanoparticles. ACS Appl Mater Interfaces 8(1):847–853. https://doi.org/10.1021/acsami.5b10192
14. Liu S, De G, Xu Y, Wang X, Liu Y, Cheng C, Wang J (2018) Size, phase-controlled synthesis, the nucleation and growth mechanisms of NaYF4:Yb/Er nanocrystals. J Rare Earths 36(10):1060–1066. https://doi.org/10.1016/j.jre.2018.01.025
15. Wang X, Yang J, Sun X, Yu H, Yan F, Meguellati K, Cheng Z, Zhang H, Yang YW (2018) Facile surface functionalization of upconversion nanoparticles with phosphoryl pillar[5] arenes for controlled cargo release and cell imaging. Chem Commun (Camb) 54(92):12990–12993. https://doi.org/10.1039/c8cc08168a
16. Dai Y, Bi H, Deng X, Li C, He F, Ma P, Yang P, Lin J (2017) 808 nm near-infrared light controlled dual-drug release and cancer therapy in vivo by upconversion mesoporous silica nanostructures. J Mater Chem B 5(11):2086–2095. https://doi.org/10.1039/c7tb00224f
17. Zhang T, Lin H, Cui L, An N, Tong R, Chen Y, Yang C, Li X, Liu J, Qu F (2016) Near infrared light triggered reactive oxygen species responsive upconversion nanoplatform for drug delivery and photodynamic therapy. Eur J Inorg Chem 2016(8):1206–1213. https://doi.org/10.1002/ejic.201501320
18. Zhang Y, Yu Z, Li J, Ao Y, Xue J, Zeng Z, Yang X, Tan TT (2017) Ultrasmall-superbright neodymium-upconversion nanoparticles via energy migration manipulation and lattice modification: 808 nm-activated drug release. ACS Nano 11(3):2846–2857. https://doi.org/10.1021/acsnano.6b07958
19. Yang G, Yang D, Yang P, Lv R, Li C, Zhong C, He F, Gai S, Lin J (2015) A single 808 nm near-infrared light-mediated multiple imaging and photodynamic therapy based on titania coupled upconversion nanoparticles. Chem Mater 27(23):7957–7968. https://doi.org/10.1021/acs.chemmater.5b03136
20. Xu F, Zhao Y, Hu M, Zhang P, Kong N, Liu R, Liu C, Choi SK (2018) Lanthanide-doped core-shell nanoparticles as a multimodality platform for imaging and photodynamic therapy. Chem Commun (Camb) 54(68):9525–9528. https://doi.org/10.1039/c8cc05057k
21. Ding X, Liu J, Liu D, Li J, Wang F, Li L, Wang Y, Song S, Zhang H (2017) Multifunctional core/satellite polydopamine@Nd3+−sensitized upconversion nanocomposite: a single 808 nm near-infrared light-triggered theranostic platform for in vivo imaging-guided photothermal therapy. Nano Res 10(10):3434–3446. https://doi.org/10.1007/s12274-017-1555-x
22. Wang X, Valiev RR, Ohulchanskyy TY, Agren H, Yang C, Chen G (2017) Dye-sensitized lanthanide-doped upconversion nanoparticles. Chem Soc Rev 46(14):4150–4167. https://doi.org/10.1039/c7cs00053g
23. Chen G, Damasco J, Qiu H, Shao W, Ohulchanskyy TY, Valiev RR, Wu X, Han G, Wang Y, Yang C, Agren H, Prasad PN (2015) Energy-cascaded Upconversion in an organic dye-sensitized core/shell fluoride nanocrystal. Nano Lett 15(11):7400–7407. https://doi.org/10.1021/acs.nanolett.5b02830
24. Yin D, Liu Y, Tang J, Zhao F, Chen Z, Zhang T, Zhang X, Chang N, Wu C, Chen D, Wu M (2016) Huge enhancement of upconversion luminescence by broadband dye sensitization of core/shell nanocrystals. Dalton Trans 45(34):13392–13398. https://doi.org/10.1039/c6dt01187j
25. Hazra C, Ullah S, Serge Correales YE, Caetano LG, Ribeiro SJL (2018) Enhanced NIR-I emission from water-dispersible NIR-II dye-sensitized core/active shell upconverting nanoparticles. J Mater Chem C 6(17):4777–4785. https://doi.org/10.1039/c8tc00335a
26. Zou X, Xu M, Yuan W, Wang Q, Shi Y, Feng W, Li F (2016) A water-dispersible dye-sensitized upconversion nanocomposite modified with phosphatidylcholine for lymphatic imaging. Chem Commun (Camb) 52(91):13389–13392. https://doi.org/10.1039/c6cc07180e
27. Xu J, Gulzar A, Liu Y, Bi H, Gai S, Liu B, Yang D, He F, Yang P (2017) Integration of IR-808 sensitized upconversion nanostructure and MoS2 nanosheet for 808 nm NIR light triggered phototherapy and bioimaging. Small 13(36):1701841. https://doi.org/10.1002/smll.201701841
28. Andresen E, Resch-Genger U, Schaferling M (2019) Surface modifications for photon-Upconversion-based energy-transfer Nanoprobes. Langmuir 35(15):5093–5113. https://doi.org/10.1021/acs.langmuir.9b00238